Acta Pharmaceutica Sinica B 2022;12(12):4390–4406

Chinese Pharmaceutical Association
Institute of Materia Medica, Chinese Academy of Medical Sciences

Acta Pharmaceutica Sinica B

www.elsevier.com/locate/apsb
www.sciencedirect.com

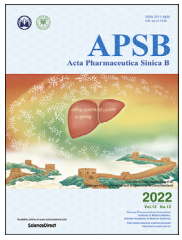

ORIGINAL ARTICLE

Sphingosine kinase 1 promotes growth of glioblastoma by increasing inflammation mediated by the NF-κB /IL-6/STAT3 and JNK/PTX3 pathways

Wan Li[a,b], Hongqing Cai[c,d], Liwen Ren[a,b], Yihui Yang[a,b], Hong Yang[a,b], Jinyi Liu[a,b], Sha Li[a,b], Yizhi Zhang[a,b], Xiangjin Zheng[a,b], Wei Tan[a,b,e,f], Guanhua Du[a,b,*], Jinhua Wang[a,b,*]

[a]*The State Key Laboratory of Bioactive Substance and Function of Natural Medicines, Beijing 100050, China*
[b]*Key Laboratory of Drug Target Research and Drug Screen, Institute of Materia Medica, Chinese Academy of Medical Science and Peking Union Medical College, Beijing 100050, China*
[c]*Department of Neurosurgery, National Cancer Center/National Clinical Research Center for Cancer/Cancer Hospital, Chinese Academy of Medical Sciences and Peking Union Medical College, Beijing 100021, China*
[d]*State Key Laboratory of Molecular Oncology, Center for Cancer Precision Medicine, National Cancer Center/National Clinical Research Center for Cancer/Cancer Hospital, Chinese Academy of Medical Sciences and Peking Union Medical College, Beijing 100021, China*
[e]*School of Pharmacy, Xinjiang Medical University, Urumqi 830011, China*
[f]*Xinjiang Institute of Materia Medica, Urumqi 830004, China*

Received 21 February 2022; received in revised form 20 June 2022; accepted 18 July 2022

KEYWORDS

Glioblastoma;
Drug target;
SPHK1;
Inflammation;

Abstract Glioblastoma (GBM) is the most challenging malignant tumor of the central nervous system because of its high morbidity, mortality, and recurrence rate. Currently, mechanisms of GBM are still unclear and there is no effective drug for GBM in the clinic. Therefore, it is urgent to identify new drug targets and corresponding drugs for GBM. In this study, *in silico* analyses and experimental data show that sphingosine kinase 1 (SPHK1) is up-regulated in GBM patients, and is strongly correlated with poor

*Corresponding author. Tel./fax: +86 10 63165184.
E-mail addresses: wjh@imm.ac.cn (Jinhua Wang), dugh@imm.ac.cn (Guanhua Du).

Peer review under responsibility of Chinese Pharmaceutical Association and Institute of Materia Medica, Chinese Academy of Medical Sciences

https://doi.org/10.1016/j.apsb.2022.09.012

NF-κB/IL-6/STAT3 signal pathway;
ATF3;
PXT3

prognosis and reduced overall survival. Overexpression of SPHK1 promoted the proliferation, invasion, metastasis, and clonogenicity of GBM cells, while silencing SPHK1 had the opposite effect. SPHK1 promoted inflammation through the NF-κB/IL-6/STAT3 signaling pathway and led to the phosphorylation of JNK, activating the JNK−JUN and JNK−ATF3 pathways and promoting inflammation and proliferation of GBM cells by transcriptional activation of PTX3. SPHK1 interacted with PTX3 and formed a positive feedback loop to reciprocally increase expression, promote inflammation and GBM growth. Inhibition of SPHK1 by the inhibitor, PF543, also decreased tumorigenesis in the U87-MG and U251-MG SPHK1 orthotopic mouse models. In summary, we have characterized the role and molecular mechanisms by which SPHK1 promotes GBM, which may provide opportunities for SPHK1-targeted therapy.

1. Introduction

Glioblastoma (GBM) is the most common and aggressive tumor of the brain, and stage IV is the most malignant type. Patients with GBM have high mortality and poor prognosis with an overall survival of less than 14.6 months[1,2]. Surgical resection combined with radiotherapy and simultaneous adjuvant temozolomide chemotherapy are the main methods for the treatment of GBM; however, few patients with GBM survive for very long. The 5-year survival rate for GBM patients is only 10%[1,2]. A high degree of heterogeneity, diffuseness and invasiveness, and the presence of brain tumor-initiating cells resistant to chemotherapy and radiotherapy are the major obstacles for the development of effective treatments[3−6]. Therefore, identifying the key driving factors for progression of GBM could provide in-depth understanding of the disease and serve as predictors for prognosis and targets for precise treatment.

Sphingolipids are one of the main lipid families in mammalian cells with a wide range of functions as components of the cell membrane, in cell−cell recognition, and in signal transduction[7]. Key molecules in the sphingolipid metabolic pathway play critical roles in the progress of inflammatory diseases and cancers. Sphingosine-1-phosphate (S1P) is an important mediator that is phosphorylated by SPHK1 and SPHK2, and functions through intracellular action or binding to the S1P receptor 1−5 (S1PR1−5, G protein-coupled receptor) on the cell surface. The SPHK1/S1P/S1PR axis modulates numerous cellular processes including proliferation, invasion, metastasis, and angiogenesis. SPHK1, the key kinase in the SPHK1/S1P/S1PR axis, was shown to be upregulated in many different cancer types, such as breast, gastric, lung, colon, liver, and GBM. The increased expression of SPHK1 was associated with a poor overall survival in patients with GBM as well as those with breast[8] and lung cancers[9]. However, its functional roles and the mechanisms of SPHK1 action in GBM have not yet been described.

Since the nineteenth century, inflammation has been correlated with the development and progression of cancer[10,11]. Chronic inflammation increases the risk of developing various types of cancer in epidemiological studies[12]. In glioma, surgical resection of glioma tissue is often accompanied by obvious local brain inflammation, up-regulation of inflammatory factor levels, and activation of inflammatory signaling pathways[13,14]. Thus, targeting transcription factors or kinases related to inflammation has emerged as a promising therapy for cancers[15]. SPHK1 is a sphingosine kinase that plays a key role in the regulation of inflammation in various types of cancer. Previous studies showed that SPHK1 was upregulated in GBM patients and correlated with a poor prognosis[16,17]. However, how SPHK1 could promote progression of GBM through inflammatory pathways and its specific mechanisms have not been investigated.

In this study, we measured the expression of SPHK1 in patients with GBM and investigated its function in GBM cells and in nude mice with xenografted GBM tumors. Our results showed that SPHK1 promoted proliferation and metastasis of GBM cells. Transcriptome data indicates that SPHK1 promotes inflammation through the NF-κB/IL-6/STAT3 signaling pathway. The *PTX3* gene, which is a biomarker for inflammatory conditions and is involved in regulating inflammation and complement activation, was also upregulated by overexpression of SPHK1. In addition, SPHK1 activated the JNK/JUN and JNK/ATF3 pathways that further promoted inflammation and growth of GBM cells by activating PTX3. More importantly, SPHK1 also interacted with PTX3 to form a positive feedback loop to reciprocally increase their expression in GBM cells. Thus, SPHK1 may prove to be a useful drug target for the treatment of GBM.

2. Methods

2.1. Cell culture

The human GBM cell lines, A172, U87-MG, T98G and U251-MG, were obtained from Procell Life Science & Technology Co., Ltd. (Wuhan, China). The normal human glial cell line, HEB, and the GBM cell lines, U138-MG, BT325, and TJ905, were obtained from GuangZhou Jennio Biotech Co., Ltd. (Guangzhou, China). The human GBM cell line, SF268, was obtained from the Chinese Academy of Sciences (Beijing, China). All cells were maintained in DMEM (Gibco, Carlsbad, CA, USA) supplemented with 10% FBS (Procell Life Science &Technology Co., Ltd.) and incubated in 5% CO_2 in a humidified incubator at 37 °C.

2.2. Establishment of stable cell lines

The human full-length SPHK1 or PTX3 cDNA clone (Myc-DDK-tagged) was purchased from OriGene Technologies (Rockville, USA). SPHK1 small hairpin RNAs (SPHK1 shRNAs) were purchased from Hanbio Biotechnology (Shanghai, China), and the sequences of SPHK1 shRNA1, shRNA2 and shRNA3 are listed in Supporting Information Table S1. Stable cell clones with high SPHK1/PTX3 expression (U251-MG SPHK1/PTX3) and

corresponding controls were selected by culturing with G418 at a concentration of 400 μg/mL for about 1.5 months. The stable low SPHK1 expression (U87-MG SPHK1 shRNA1, U87-MG SPHK1 shRNA2) cell lines and a corresponding control were selected with puromycin at a concentration of 2 μg/mL for 14 days. These stable cell lines were used to assess the functional roles of SPHK1 in GBM cells, such as proliferation (CCK-8 assay), migration and invasion (Transwell assays), clonogenicity, and cell growth in 3D Matrigel.

2.3. *Cell proliferation, migration and invasion assays*

The CCK-8 (Beyotime, Shanghai, China) assay was used to determine cell proliferation[18]. Briefly, 3×10^3 cells (per well) were seeded in a 96-well plate and incubated for 0, 24, 48, 72 and 96 h. The absorbance of each well at 450 nm was quantified using a SpectraMax M5 (Molecular Devices, LLC., San Jose, CA, USA). Costar 24-Transwell Plates (Corning, New York, USA) with 8 μm polycarbonate membranes were used to measure cell migration and invasion ability of GBM cells[19]. For the invasion assay, the bottom polycarbonate membrane was coated with 13% Matrigel (Corning, NY, USA). Cells were harvested and re-suspended in FBS-free medium, and 5×10^4 cells (about 300 μL) were added to the upper chamber. One mL of complete medium was added to the lower chamber. After 18 h (migration) or 24 h (invasion), the cells that had traversed the polycarbonate membrane were fixed with 4% paraformaldehyde (4% PFA) for 15 min, stained with 1% crystal violet solution for 20 min, then washed with water until no more color was seen. The non-traversed cells were gently wiped off with a cotton swab and the number of traversed cells was counted under a visible-light microscope (Nikon, Tokyo, Japan).

2.4. *Colony formation assay and 3D matrigel culture*

Six-well plates were used to perform the colony formation assay. Two mL of 0.7% low-melting temperature agarose in DMEM containing 10% FBS was added to each well of a 6-well plate to serve as the bottom layer and the top layer contained 3000 cells suspended in 1 mL of 0.35% low melting-temperature agarose in DMEM with 10% FBS. The plates were incubated for 2−4 weeks. Lastly, the clones were stained with 200 μL of MTT solution (5 mg/mL) and the number of clones was counted. The 3D Matrigel culture was carried out in 96-well plates with each well containing 50 μL of Matrigel (Corning, NY, USA) and 50 μL of complete medium plus 1000 cells. After culturing for two weeks, the sizes of the colonies were determined under a visible-light microscope (Nikon, Tokyo, Japan).

2.5. *Protein immunoassays by Western blot*

For total protein extraction, cells were disrupted in RIPA (Applygen, Beijing, China) lysis buffer containing a Protease and Phosphatase Inhibitor Cocktail (Beyotime, Shanghai, China) at 4 °C for 30 min. The cell lysates were centrifuged at 12,000 × *g* for 10 min at 4 °C and the supernatants were collected. The BCA Protein Assay Kit (Beyotime, Shanghai, China) was used to quantify the protein concentrations of each sample. Protein aliquots were separated on 10% SDS-PAGE and proteins were transferred to polyvinylidenedifluoride (PVDF) membranes (Millipore, Billerica, USA). The blots were then blocked in 5% fat-free milk for 1 h at room temperature and incubated with primary antibodies at the recommended dilutions with gentle agitation overnight at 4 °C. The primary antibodies included SPHK1, ATF3, p-NF-κB-p65, NF-κB-p65, p-STAT3, STAT3, p-p38-MAPPK, p38-MAPPK, p-ERK1/2, ERK1/2, p-JNK, JNK, p-JUN and JUN (Cell Signaling Technology, Danvers, USA), PTX3 and GAPDH (Proteintech, Rosemont, USA). After washing, the blots were incubated with the corresponding HRP-linked secondary antibody (Cell Signaling, Danvers, USA). Stained bands were visualized with a Tanon 5200 Automatic Imaging System (Tanon, Shanghai, China) using a hypersensitive ECL solution (Applygen, Beijing, China).

2.6. *Differential gene expression analysis by real-time quantitative PCR (RT-qPCR)*

Total RNA was extracted from cells with TRIzol reagent (Invitrogen, Carlsbad, USA) and cDNA was synthesized using the MonScriptTM RT lll All-in-One Mix (Monad Biotech, Wuhan, China). The AceQ Universal SYBR qPCR Master Mix (Vazyme Biotech, Nanjing, China) was used with RT-qPCR to determine the relative expression of selected differentially expressed genes (DEGs) in a CFX 96 thermocycler (Bio-Rad, Hercules, CA, USA). The primers used in RT-qPCR are listed in Supporting Information Table S2.

2.7. *Transcriptome sequencing and functional enrichment analyses for DEGs*

The U251-con and U251-SPHK1 cells were collected and lysed with TRIzol reagent (Invitrogen, Carlsbad, USA) and prepared for transcriptome sequencing by Novogene Co., Ltd. (Beijing, China). The total RNA was qualified on the Agilent 2100 Bioanalyzer System and libraries were generated using NEBNext® Ultra™ RNA Library Prep Kit for Illumina® following manufacturer's instructions. The llumina PE150 libraries were normalized, pooled and sequenced on the IlluminaHiSeq™ Nova sequencing platform (Illumina Inc., San Diego, CA, USA). For mapping the Illumina RNA-seq reads, HISAT2 v2.0.5 was used to align the FASTQ data to the reference genome (GRh38). The reads of each gene were counted using HTSeq v0.6.1, then, the fragments per kilobase per million (FPKM) were calculated to quantify the expression level of the corresponding gene. DEGs between SPHK1 overexpression and control groups were identified by the DESeq2 R package v1.16.1. The DAVID website (https://david.ncifcrf.gov/home.jsp) was used to perform the gene ontology (GO) and Kyoto Encyclopedia of Genes and Genomes (KEGG) enrichment analysis of DEGs.

2.8. *Immunohistochemistry*

Glioma tissue arrays were purchased from Xi'an Alenabio Biological Technology Co., Ltd. (Xi'an, China). Immunohistochemical staining was carried out as previously described[20,21]. In brief, the arrays were dried, deparaffinized, and rehydrated. Subsequently, the slides were immersed in boiling 10 mmol/L sodium citrate buffer (pH 6.0) for 20 min for antigen retrieval. The slides were then incubated with 3% hydrogen peroxide solution at room temperature for 10 min to block the activity of endogenous peroxidase. Sections were blocked with 10% normal goat serum for 30 min, and then incubated with SPHK1/PTX3 primary antibody (1:50 dilution; Proteintech, Rosemount, IL, USA) overnight at 4 °C. Negative controls were incubated with PBS alone. The

IHC Detection System (ZSGB-BIO, Beijing, China) was used for the subsequent experiments. Sections were counterstained with hematoxylin and mounted with neutral gum. The semi-quantitative analysis of stained slides was performed according to the Remmele and Stegner immunoreactivity score (IRS)[36,37] under a visible-light Microscope (Nikon, Tokyo, Japan).

2.9. Edu DNA synthesis assay

The DNA synthesis assay was performed using the Cell-Light EdU Apollo 567 *In Vitro* Imaging Kit (RIBOBIO, Guangzhou, China) according to the manufacturer's instructions[22]. Briefly, cells were seeded in 96-well plates at a density of 1×10^5 per well, and 24 h later, 50 μmol/L EdU was added to the culture medium and incubated for 4−6 h. The cells were then fixed for 30 min in 4% paraformaldehyde, permeabilized for 10 min using 0.5% Triton-X 100, and stained for 30 min with 10 μmol/L Apollo 567. DNA was stained with Hoechst 33342 for 30 min and cells were imaged with a High-Resolution Digital Imaging System (Thermo Fisher Scientific, Waltham, USA).

2.10. Chromatin immunoprecipitation (ChIP) assay

U251 cells were transfected with ATF3-overexpressing or control plasmids and 24 h later, the cells were collected and processed using the SimpleChIP® Enzymatic Chromatin IP Kit (9002, Signaling Technology, Danvers, MA, USA). Cells were cross-linked in 1% formaldehyde and then quenched using 0.125 mol/L glycine. Nuclear lysates were digested by micrococcal nuclease and incubated with control IgG or anti-ATF3 antibody. The genomic DNA of interest was precipitated by magnetic beads, reverse-crosslinked, purified by spin column, and used as template for RT-qPCR analysis.

2.11. Co-immunoprecipitation (Co-IP) assay

U251-MG cells were transfected with SPHK1 or PTX3 plasmids, and 24 h later the cells were collected and disrupted in lysis buffer. Cell lysates were incubated with control IgG or SPHK1/PTX3 primary antibodies with gentle agitation overnight at 4 °C. Then, 25 μL of protein A/G agarose beads were added to lysates and incubated for 2 h. The agarose beads were pelleted and washed five times. Immunoprecipitated proteins were eluted by heating at 95 °C for 10 min. The protein levels of SPHK1 and PTX3 were determined by Western blot.

2.12. In vivo GBM models

2.12.1. Animals

Six-week-old BALB/c *nu/nu* mice (female) were used in this study. The mice were purchased from Beijing Vital River Laboratory Animal Technology Co., Ltd. (Beijing, China). All mice were housed in a barrier system (12-h light/dark cycle, temperature 22 ± 2 °C, relative humidity 50 ± 10%) with free access to food and water. All experimental procedures were performed according to the principles of the NIH Guide for the Care and Use of Laboratory Animals and the experimental procedures were approved by the animal ethics committee of the Institute of Materia Medica, CAMS & PUMC (Beijing, China).

2.12.2. Xenograft tumor model

U251-MG Con, U251-MG SPHK1, U87-MG Sh-NC, U87-MG Sh-SPHK1-1, and U87-MG Sh-SPHK1-2 cells (a total of 1×10^7 cells) were collected and subcutaneously injected into the right flank of the mice. After tumor formation, the length and width were measured with a digital Vernier caliper and the tumor volume was calculated using Eq. (1):

$$V\ \left(\mathrm{mm}^3\right) = 0.5 \times L \times W^2 \tag{1}$$

where L is the length in mm and W is the width in mm of the tumor. After 28 days, all the mice were euthanized, the tumors were weighed, and the tumor tissues were collected for examination.

2.12.3. GBM orthotopic model

BALB/c *nu/nu* mice were anesthetized with sodium pentobarbital (60 mg/kg, i. p.) and fixed in a stereotaxic apparatus[23]. A small hole (3 mm to the right and 0.5 mm anterior to the bregma) was drilled through the skull and U87-MG or U251-MG Con/U251-MG SPHK1 cells (2×10^5 cells/μL) were transplanted into the right striatum of the mice at a depth of 3.3 mm below the skull. Aliquots of 5 μL of cell suspension were slowly injected at a rate of 1 μL/min into the striatum of the mice. For the U87-MG GBM orthotopic model, at five days after the surgery, 10 mg/kg of PF543 was administered to the mice on alternate days for 21 days. For the U251-MG Con/U251-MG SPHK1 glioma orthotopic model, at two weeks after the surgery, 10 mg/kg PF543 was administered to mice on alternate days for 21 days. At the end of the experiment, magnetic resonance imaging was used to determine the tumor volume in the mice.

2.13. Statistical analysis

The results are presented as mean ± standard deviation (SD). Student's t test was used to evaluate differences between two groups and one-way ANOVA to analyze differences among different groups. The difference was considered significant at $P < 0.05$.

3. Results

3.1. SPHK1 is highly expressed in GBM and associated with clinical characteristics of patients with GBM

To evaluate the expression level of SPHK1 in GBM, we measured mRNA expression of *SPHK1* in normal cells and tissues compared to GBM cells and tissues using GEPIA, the Broad Institute, the Human Protein Atlas, Oncomine, and TCGA databases by *in silico* methods. Results show that the mRNA expression of *SPHK1* was higher in GBM than in normal tissues (Fig. 1A and B). In addition, SPHK1 was highly expressed in some GBM cells, such as U138-MG, A172, and U87-MG (Fig. 1C), and the mRNA expression of *SPHK1* was higher in GBM tissues than in normal and other types of glioma tissues (Fig. 1D and E). These data demonstrate that SPHK1 was highly expressed in GBM. To clarify why SPHK1 was highly expressed in GBM, we searched transcription factors in the promoters of SPHK1 by using PROMO website and checked if they were associated with GBM. We found that 78 transcription factors could bind the promoter of *SPHK1* (Supporting Information Fig. S1). Among 78 transcription factors, *ATF3*, *CMYB*, *HOXD9*, *HOXD10*, *ATF1*, *AR*, *LEF1*, *IRF2*, *ELF1*,

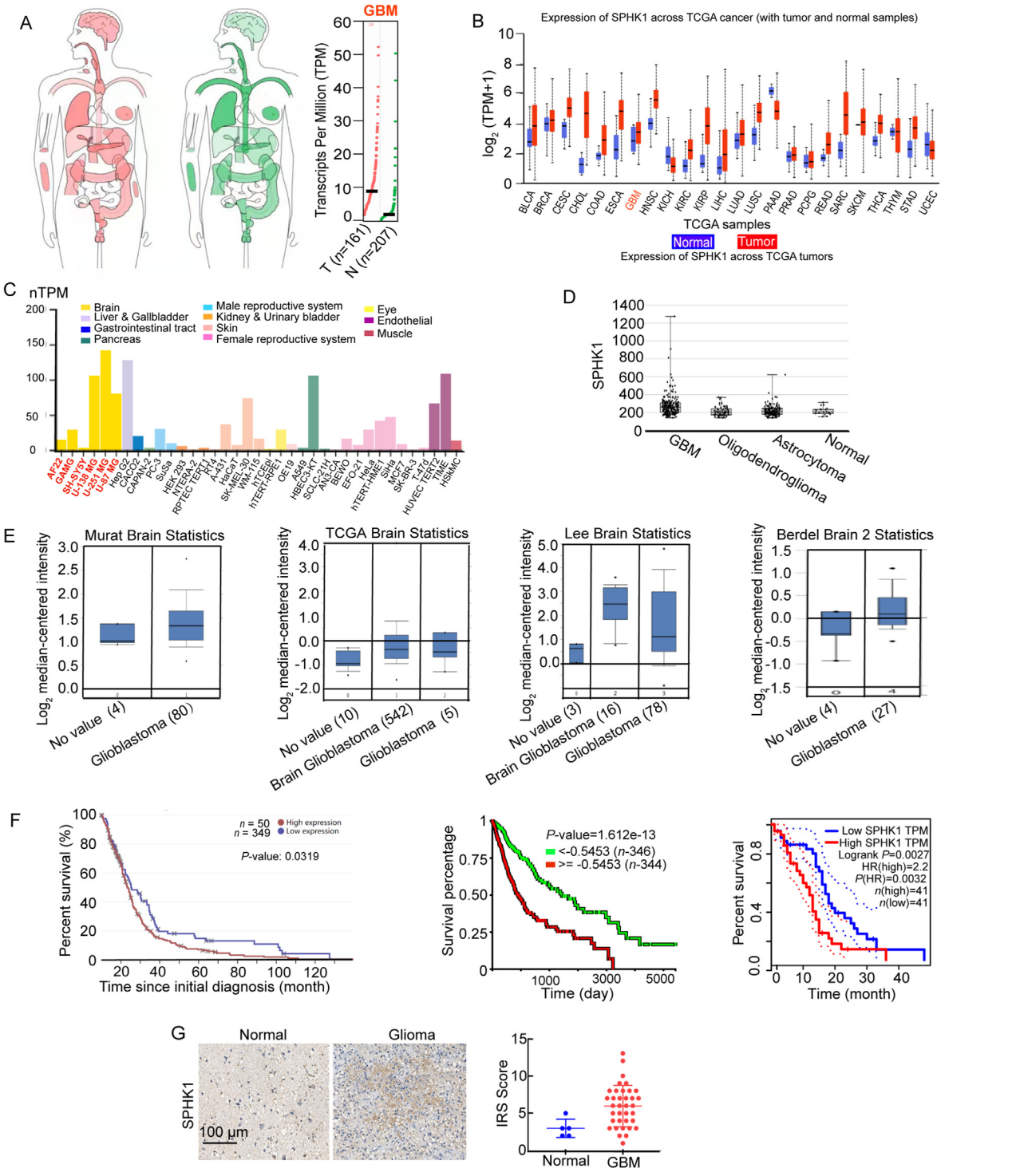

Figure 1 SPHK1 is highly expressed in patients with glioma and associated with clinical features. Data from (A) GEPIA (http://gepia.cancer-pku.cn/), (B) Broad Institute (http://gdac.broadinstitute.org/.), (C) Human Protein Atlas (http://www.proteinatlas.org/), (D) Betastasis (https://www.betastasis.com/), and (E) Oncomine website (www.oncomine.org) shows that the expression of SPHK1 is higher in GBM tissues and cells than in normal tissues or other kinds of tumor. (F) Data from Betastasis website (https://www.betastasis.com/), UCSC Xena website (http://xena.ucsc.edu/) and GEPIA website (http://gepia.cancer-pku.cn/) shows that the overall survival rate of patients with high SPHK1 expression is lower than that of patients with low SPHK1 expression. (G) Immunohistochemical analysis shows that the expression of SPHK1 is significantly higher in GBM tissues than in normal brain tissues.

XBP1, *CEBPB*, *CEBP3*, *GATA3*, *RELA*, *TP53*, *WT1* are associated with malignant GBM.

In silico analysis was used to determine the relationship between SPHK1 expression and survival rate of patients with GBM. As shown in Fig. 1F, GBM patients with high expression of SPHK1 had a lower overall survival rate than those with low expression of SPHK1, suggesting that SPHK1 could be a potential drug target for treating GBM. To determine if expression of SPHK1 is associated with the clinical characteristics of patients with GBM, we analyzed the expression of SPHK1 in paraffin-embedded GBM tissues and adjacent normal tissues. Our results show that SPHK1 expression was significantly higher in GBM tissues than in normal brain tissues (Fig. 1G). These results demonstrate that SPHK1 is highly expressed in GBM, and that SPHK1 expression is associated with poor outcomes in GBM patients.

3.2. *SPHK1 plays an important role in GBM cells*

To investigate the role of SPHK1 in GBM cells, loss- and gain-of function assays were carried out (Fig. 2A). Firstly, we measured the mRNA and protein expressions of SPHK1 and S1P levels in a panel of GBM cell lines and found the lowest expression in U251-MG cells and the highest expression in U87-MG cells (Fig. 2B and Supporting Information Fig. S2). Stable U251-MG cells with overexpression of SPHK1 were established by the sub-cloning of full-length human *SPHK1* cDNA into the pCMV6 vector (pCMV6-SPHK1), which was named U251-MG SPHK1. Stable

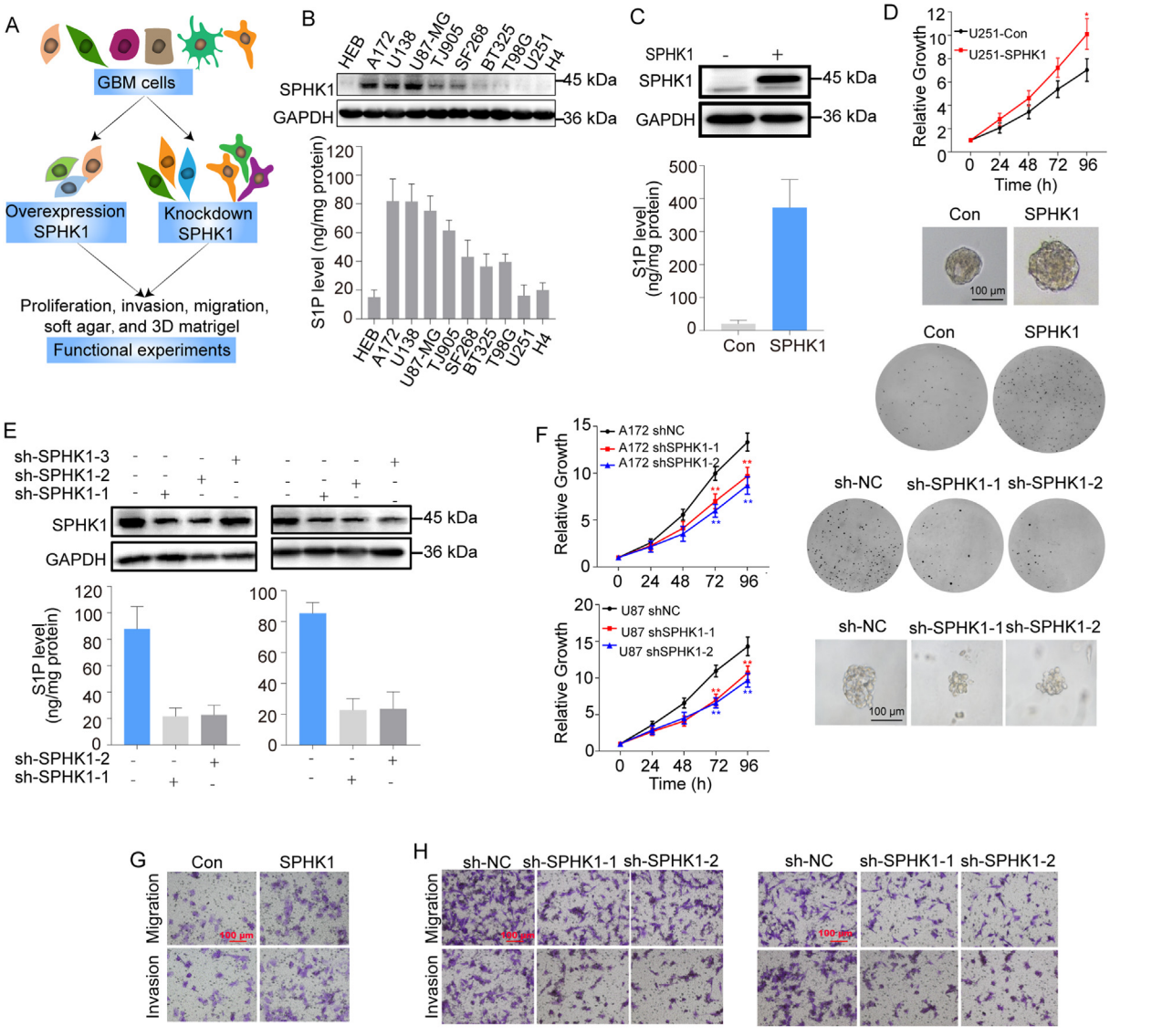

Figure 2 SPHK1 promotes proliferation, migration, invasion, colony formation, and growth of GBM cells. (A) Approach for defining the function of SPHK1 in GBM cells. (B) Western blot and ELISA results show that the protein levels of SPHK1 and S1P were higher in A172 and U87-MG cells and lower in U251-MG and H4 cells. (C) Overexpression of SPHK1 in U251 cells. (D) Overexpression of SPHK1 promotes proliferation, colony formation, and cell growth in 3D Matrigel in U251 cells. (E) Knockdown of SPHK1 in U87-MG and A172 cells. (F) Knockdown of SPHK1 inhibited proliferation, colony formation, and cell growth in 3D Matrigel in U87-MG and A172 cells. (G) Overexpression of SPHK1 promoted migration and invasion of U251-MG cells. (H) Knockdown of SPHK1 had the opposite effects in U87-MG and A172 cells. The data are presented as mean ± SD, and the experiments were performed in triplicate.

U87-MG cells with low SPHK1 expression were established using RNA interference with *SPHK1* shRNAs (pHBLV-shSPHK1 1/2), and were named U87-MG shSPHK1-1 and U87-MG shSPHK1-2, respectively. Overexpression of SPHK1 in U251-MG cells promoted cell proliferation (Fig. 2C and D) and increased clonogenicity and growth in both soft agar and 3D Matrigel (Fig. 2D, and Supporting Information Fig. S3A), whereas knockdown of SPHK1 in U87-MG and A172 cells reduced proliferation (Fig. 2E), clonogenicity and growth (Fig. 2F and Fig. S3B).

To define the role of SPHK1 in the motility of GBM cells, invasion and migration assays were carried out in U251-MG Con, U251-MG SPHK1, U87-MG shNC, U87-MG shSPHK1-1, and

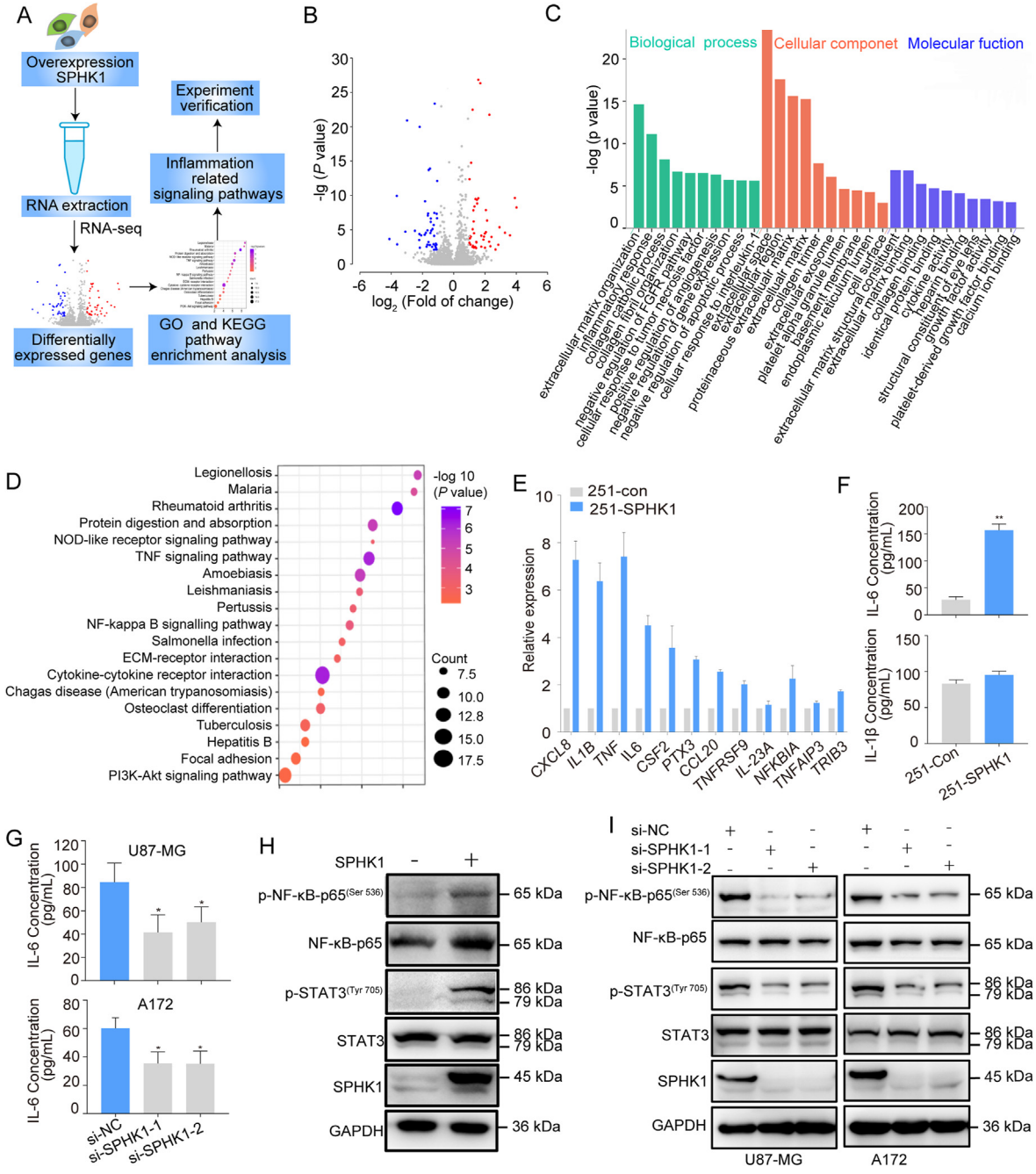

Figure 3 SPHK1 is associated with inflammatory signaling pathways. (A) Strategy for investigating the mechanisms of SPHK1. (B) Volcano plot of differentially expressed genes in U251 cells after overexpression of SPHK1 (up-regulated genes are in red; down-regulated genes are in blue; fold change $\geq$2). (C) Gene ontology analysis of DEGs after overexpression of SPHK1. (D) KEGG pathway enrichment of DEGs (fold change $\geq$2 and $P < 0.05$) (E) RT-qPCR results confirmed that the mRNA levels of key genes involved in inflammatory signaling were higher after overexpression of SPHK1 in U251-MG cells. (F) The concentration of IL-6 and IL-1β was higher in U251 cells after overexpression of SPHK1. (G) The concentration of IL-6 was lower in U87-MG and A172 cells after silencing of SPHK1. (H) The protein levels of NF-κB and STAT3 were increased in U251 cells after overexpression of SPHK1. (I) The protein levels of NF-κB and STAT3 were decreased in U87-MG and A172 cells after silencing of SPHK1. The data are presented as mean $\pm$ SD, and the experiments were performed in triplicate.

U87-MG shSPHK1-2 cell lines. As shown in Fig. 2G and Fig. S3C, overexpression of SPHK1 facilitated the migration and invasion of GBM cells, whereas knockdown of SPHK1 expression reduced cell migration and invasion of U87-MG and A172 cells (Fig. 2H, Fig. S3D and S3E). Taken together, we think that SPHK1 plays an important role in the development of GBM.

3.3. *SPHK1 increases inflammation in GBM*

To elucidate the mechanism by which SPHK1 promotes GBM development, we examined the transcriptomic sequencing after overexpression of SPHK1 in U251-MG cells to identify the differentially expressed genes (DEGs) (Fig. 3A). Compared with the U251-MG control group, a total of 72 down-regulated genes and 58 up-regulated genes were identified after overexpression of SPHK1 (Fig. 3B). Subsequently, the GO (gene ontology) and KEGG (Kyoto Encyclopedia of Genes and Genomes) pathway enrichment analyses of these DEGs were performed on the DAVID website (Fig. 3C and D). The enriched KEGG pathways included rheumatoid arthritis, TNF signaling pathway, NF-κB signaling pathway, PI3K−Akt signaling pathway, and cytokine−cytokine receptor interaction (Fig. 3D and Supporting Information Table S3). The String website using Cytoscape software was used to construct the PPI (protein−protein interaction) network (Supporting Information Fig. S4). These results suggest that SPHK1 may be involved in signaling pathways related to inflammation.

To test the results of RNA-Seq, 12 DEGs involved in inflammation-related signaling pathways were selected for validation by RT-qPCR assay (Fig. 3E). In addition, the results from an ELISA show that the level of IL-6 was increased in U251-MG SPHK1 cells and decreased in U87-MG and A172 si-SPHK1 cells (Fig. 3F and G). The results from Western blots show that the ratios of p-NF-κB-p65/NF-κB-p65 and p-STAT3/STAT3 were increased in U251-MG SPHK1 cells and decreased in U87-MG and A172 si-SPHK1 cells (Fig. 3H and I). In summary, these results confirm that SPHK1 plays an important role in regulation of inflammation-related signaling pathways.

3.4. *PTX3 is regulated by SPHK1 in GBM cells and highly expressed in GBM tissues*

To further delve into the influence of SPHK1 on the regulation of inflammation in GBM cells, we screened DEGs in U251-MG Con and U251-MG SPHK1 cells to identify inflammation-related genes that were regulated by SPHK1. In the list of DEGs from over-expression of SPHK1, *PTX3* was one of the top-ranked genes (Fig. 4A). *PTX3* encodes a secreted protein of the pentraxin protein family, which is linked to regulation of inflammation and complement activation. This gene is involved in regulating inflammation and complement activation and is a biomarker for several inflammatory conditions. The results of RT-qPCR and Western blot confirmed that both mRNA and protein expression of PTX3 were regulated by SPHK1 (Fig. 4B and C). Additionally, results from ELISAs and confocal immunofluorescence show that SPHK1 overexpression increased the expression of PTX3 in U251-MG cells (Fig. 4D and E), suggesting that PTX3 may be a downstream target of SPHK1.

To further confirm that SPHK1 regulates the expression of PTX3, we checked whether the expression of PTX3 was also high in GBM tissues using GEPIA, the Broad Institute, Oncomine, and GTEx databases. Data from GEPIA and the Broad Institute showed that PTX3 expression was higher in glioma tissues than in normal tissues (Fig. 4F) and was markedly higher in the GBM tissues than in other types of glioma (Fig. 4G). Similar results were confirmed by results from the Oncomine database (Fig. 4H and I), and data from GTEx databases also showed that PTX3 expression was highly expressed in GBM tissues independent of sample types, patient's races, ages, and p53 mutation status (Fig. 4J).

Overall, our results show that PTX3 expression was especially high in GBM relative to normal and other types of tumors. The methods of *in silico* analysis were used to investigate whether the expression of PTX3 correlated with the survival rate of GBM patients, and we found that the overall survival rate of patients with high PTX3 expression was lower than that of patients with low PTX3 expression (Fig. 4K). IHC results also show that the expression of PTX3 was obviously higher in GBM tissues than in normal brain tissues (Fig. 4L). These results, combined with the previous data showing that SPHK1 overexpression increased the expression of PTX3, support the hypothesis that PTX3 was regulated by SPHK1.

3.5. *PTX3 mediates the role of SPHK1 in GBM cells*

We found that SPHK1 increased the expression of PTX3, which was also highly expressed in GBM tissues. Therefore, we speculated that *PTX3* must be a major downstream gene of SPHK1, mediating its function in GBM cells. To test this hypothesis, we first determined if PTX3 and SPHK1 had similar functions. We measured the mRNA and protein levels of PTX3 in many GBM cell lines and found the lowest expression in U251-MG, and the highest expression in U138-MG among the GBM cell lines (Fig. 5A). Stable U251-MG cells with overexpression of *PTX3* were established by sub-cloning the full-length human *PTX3* cDNA into the pCMV6 vector (pCMV6-SPHK1) (Fig. 5B), which was named U251-MG PTX3. Stable U138-MG cells with low PTX3 expression were established using *PTX3* shRNAs (Fig. 5C), which were named U138-MG shPTX3-1 and U138-MG shPTX3-3, respectively. Overexpression of PTX3 increased metastasis and tumor spheroid formation of U251-MG cells (Fig. 5B, Supporting Information Fig. S5A and S5C), whereas knockdown of PTX3 expression in U138-MG cells had the opposite effect (Fig. 5C, Fig. S5B and S5D). Overexpression of PTX3 also increased IL-6 concentration and reduced the ratio of p-STAT3/STAT3 in U251-MG cells, whereas knockdown of PTX3 in U138-MG cells had the opposite effect (Fig. 5B and C). These results indicate that PTX3 enhanced growth and promoted the inflammatory response in GBM cells, similar to the function of SPHK1.

Next, we tested whether knockdown of PTX3 expression could rescue GBM cells by silencing PTX3 in U251-MG Con and U251-MG SPHK1 cells (Fig. 5D). Silencing *PTX3* impaired release of IL-6, colony formation, 3D growth, as well as the ratio of p-STAT3/STAT3 caused by SPHK1 in U251-MG cells (Fig. 5E−H, Fig. S5E). Furthermore, EdU and CCK-8 analyses revealed that SPHK1 promoted proliferation of U251-MG cells, while silencing PTX3 inhibited proliferation in U251-MG Con and U251-MG SPHK1 cells (Fig. 5I and J). Lastly, confocal immunofluorescence assays revealed co-localization of SPHK1 and PTX3 in the nucleus and cytoplasm in U251-MG and U87-MG cells (Fig. 5K). Our results suggest that PTX3 mediated the activity of SPHK1 in GBM cells.

3.6. *SPHK1 enhances PTX3 expression through the ATF3 pathway*

To investigate how SPHK1 regulated the expression of PTX3, we tested several transcription factors to determine if they were

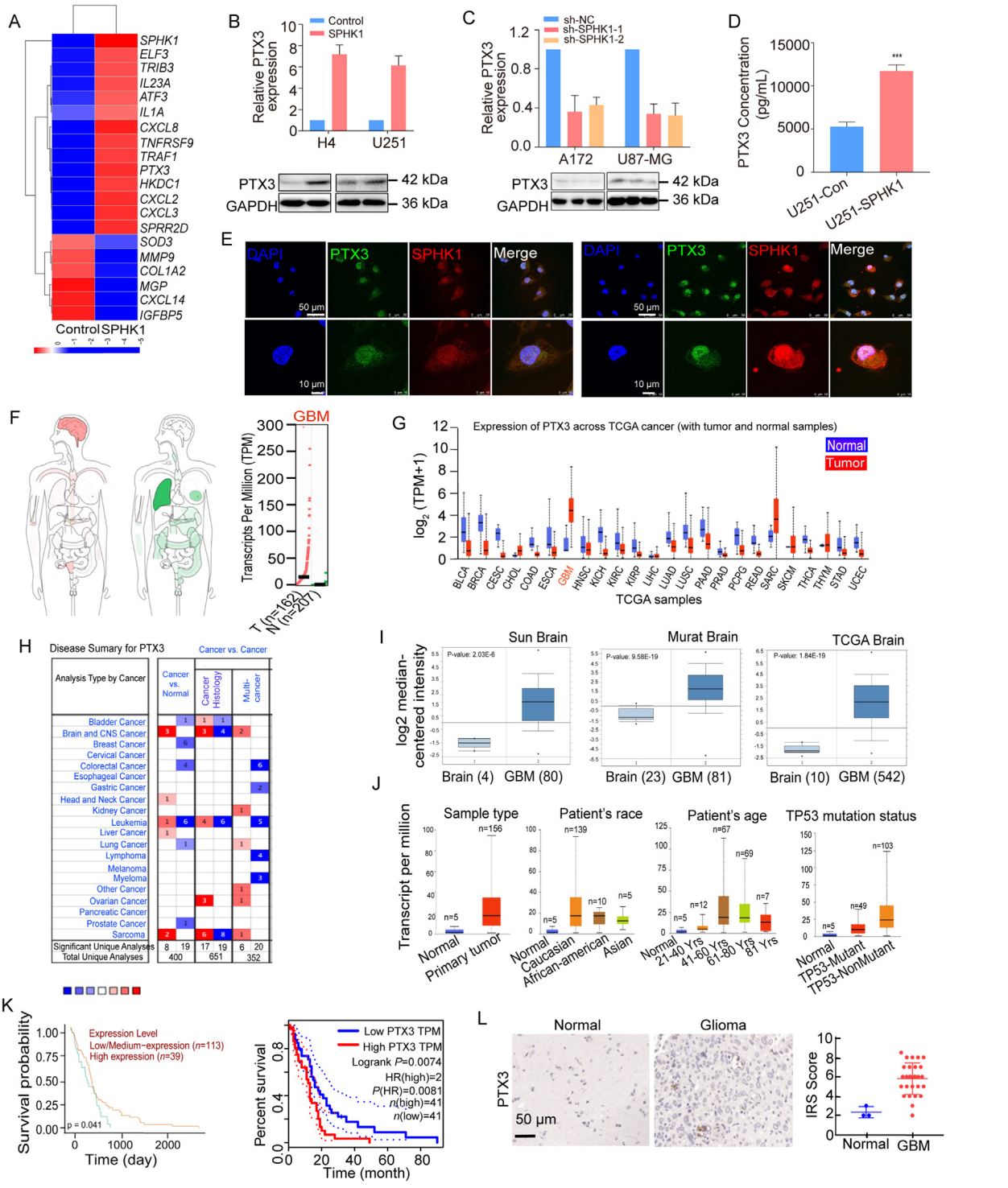

Figure 4 PTX3 is regulated by SPHK1 and promotes inflammation and proliferation of GBM cells. (A) Heatmap of top-ranked DEGs after SPHK1 overexpression in U251 cells. (B) The mRNA and protein expression of PTX3 was increased in U251 cells after overexpression of SPHK1. (C) The mRNA and protein expression of PTX3 was decreased in A172 and U87-MG cells after knockdown of SPHK1. (D) The concentration of PTX3 was increased in U251 cells after overexpression of SPHK1. (E) Confocal immunofluorescence staining of SPHK1 and PTX3 showed that protein expression of PTX3 was increased after overexpression of SPHK1. (F) Data from GEPIA website (http://gepia.cancer-pku.cn/) shows that expression of PTX3 is higher in GBM tissues than in healthy tissues. (G) Data from the Broad Institute website (http://gdac.broadinstitute.org/.) shows that the expression of PTX3 is higher in GBM tissues than in healthy tissues. Data from (H, I) Oncomine (www.oncomine.org) and (J) UALCAN (http://ualcan.path.uab.edu/index.html) website shows that the expression of PTX3 is higher in GBM tissues than in normal tissues. (K) Data from Betastasis (https://www.betastasis.com/) and GEPIA (http://gepia.cancer-pku.cn/) website shows that the overall survival rate in patients with high expression of PTX3 is lower than in those with low expression of PTX3. (L) Immunohistochemical results indicate that the expression of PTX3 was higher in GBM tissues than in normal tissues. Representative images showing the expression of PTX3 in GBM and adjacent normal tissues. The data are presented as mean ± SD, and the experiments were performed in triplicate.

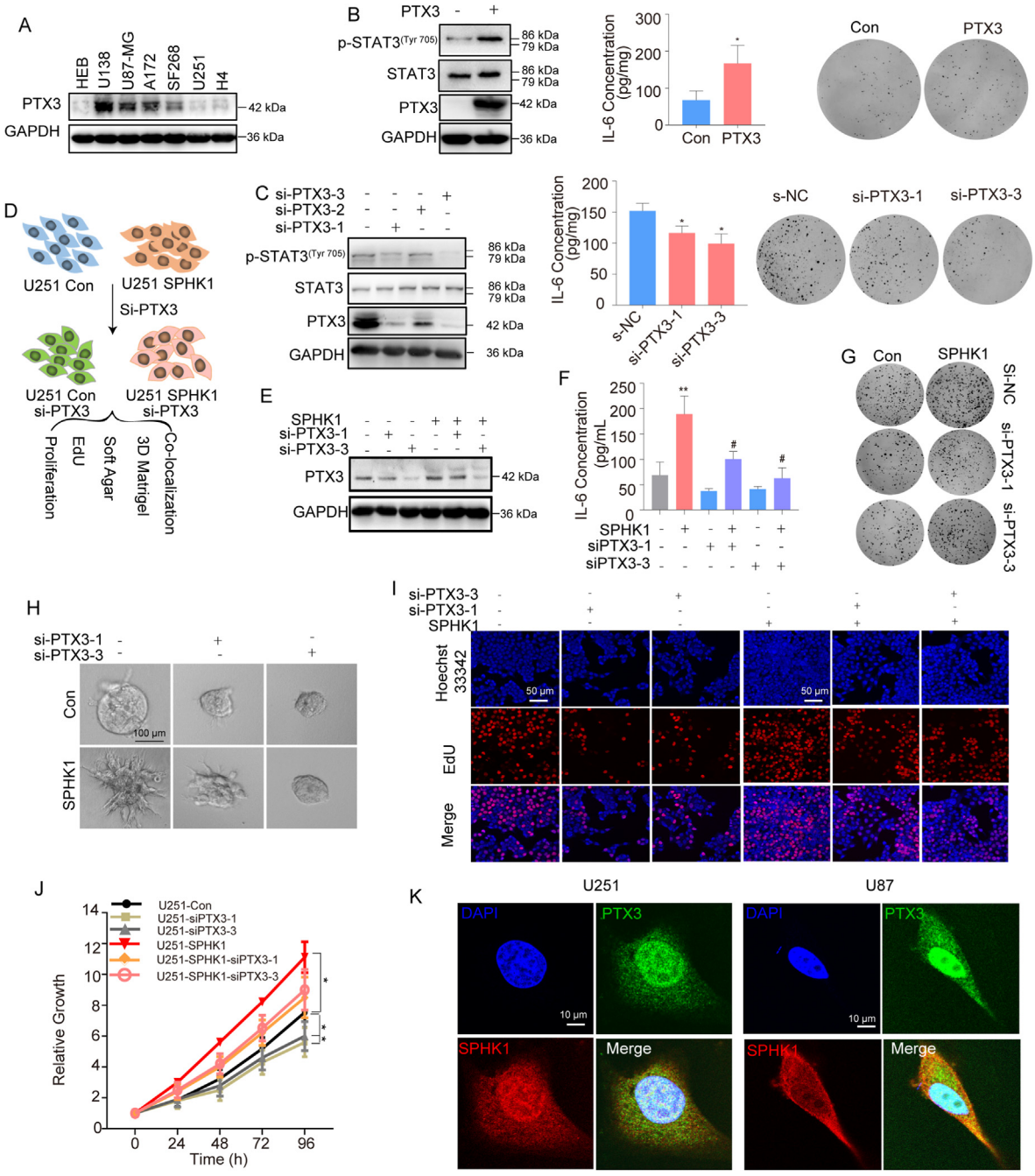

Figure 5 PTX3 mediates the function of SPHK1 in GBM cells. (A) Protein expression of PTX3 in normal *vs*. GBM cells. (B) Overexpression of PTX3 increases the ratio of p-STAT3/STAT3 and the release of IL-6, and promotes colony formation of U251-MG cells. (C) Knockdown of PTX3 decreases the ratio of p-STAT3/STAT3 and the release of IL-6, and inhibits colony formation of U138-MG cells. (D) Strategy for investigating PTX3 function after overexpression of SPHK1. (E) Knockdown of PTX3 in U251 cells with overexpressed SPHK1. (F) ELISA results show that silencing *PTX3* impairs release of IL-6 caused by overexpression of SPHK1 in U251-MG cells. (G) Silencing *PTX3* decreases colony formation caused by overexpression of SPHK1 in U251-MG cells. (H) Silencing *PTX3* inhibits growth of U251 cells in 3D Matrigel caused by overexpression of SPHK1. EdU analysis (I) and CCK-8 analysis (J) show that silencing PTX3 inhibits proliferation of U251 cells caused by overexpression of SPHK1. (K) Results from confocal immunofluorescence show that SPHK1 and PTX3 were co-localized in the cytoplasm and nuclei in U251-MG and U87-MG cells. The data are presented as mean ± SD, and the experiments were performed in triplicate.

involved in the regulation of PTX3 expression by SPHK1 (Fig. 6A). The PROMO website (http://alggen.lsi.upc.es/cgi-bin/promo_v3/promo/promoinit.cgi?dirDB=TF_8.3.) was used to identify putative transcription factors that might regulate the expression of PTX3, and we found 71 transcription factors that might be involved in PTX3 regulation (Supporting Information Fig. S6A). By screening the transcriptome data after overexpression of SPHK1 in U251-MG cells, we identified IRF-1,

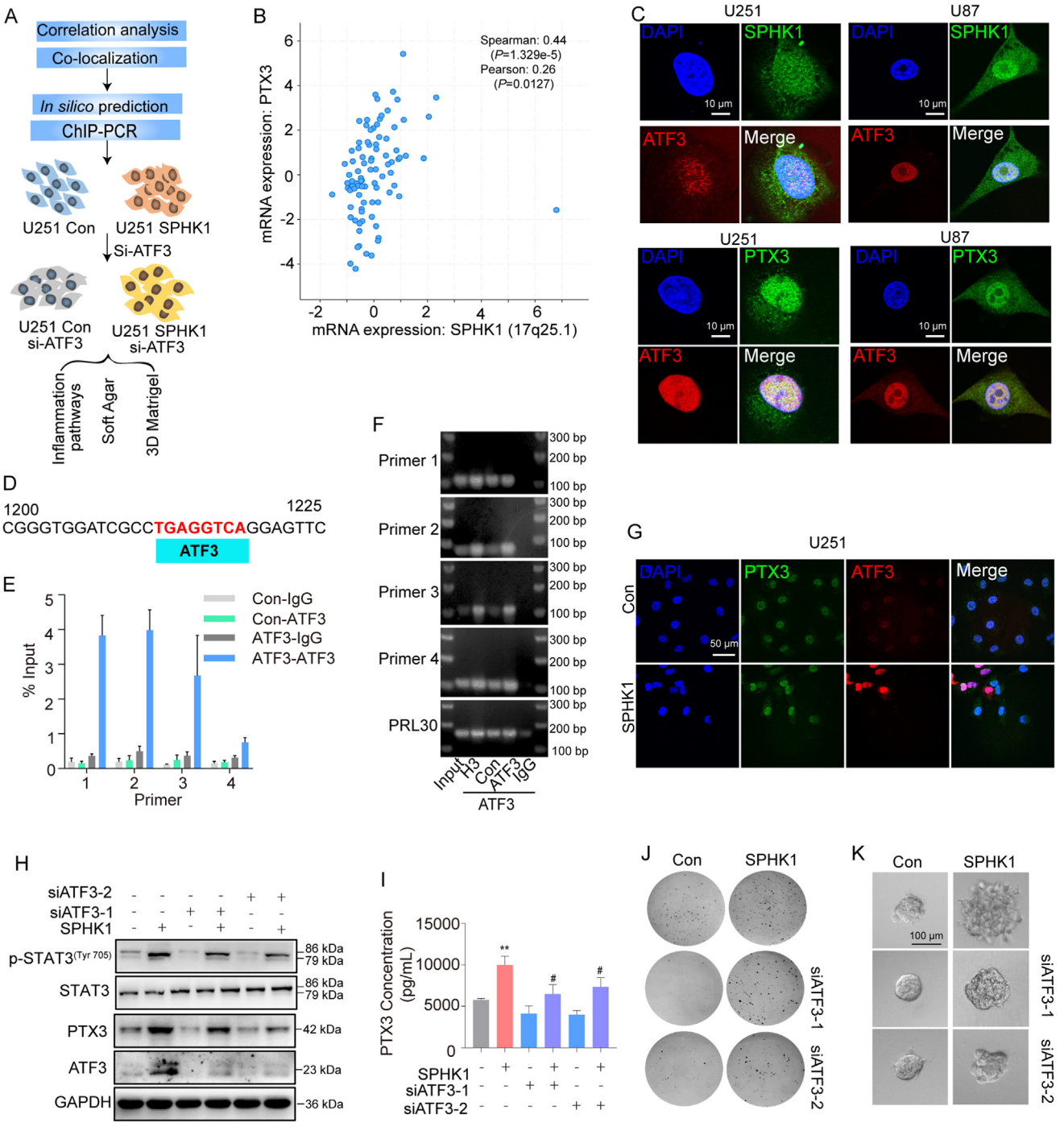

Figure 6 SPHK1 promotes the expression of PTX3 through ATF3. (A) Strategy for identifying ATF3 as the key transcription factor in regulating the expression of PTX3. (B) *In silico* analysis of TCGA data shows that SPHK1 is highly correlated with PTX3. (C) Results from confocal immunofluorescence show that SPHK1 and ATF3 or ATF3 and PTX3 are co-localized in the nucleus in U251-MG and U87-MG cells. (D) Prediction of the binding site of ATF3 in the promoter region of PTX3 using PROMO website (http://alggen.lsi.upc.es/cgi-bin/promo_v3/promo/promoinit.cgi?dirDB=TF_8.3.). (E) ChIP-qPCR analysis shows that ATF3 binds to PTX3 promoter in U251 cells. (F) Gel electrophoresis of ChIP-qPCR products. (G) Confocal immunofluorescence assay revealing that overexpression of ATF3 increases PTX3 expression in U251-MG cells. (H) Western blot results show that silencing ATF3 impairs the effects of SPHK1 on the expression of ATF3, PTX3, and the ratio of p-STAT3/STAT3 in U251-MG cells. Silencing ATF3 impairs the effect of SPHK1 on the expression of PTX3 (I), colony formation (J), 3D growth (K) in U251-MG cells. The data are presented as mean ± SD, and the experiments were performed in triplicate.

ATF-3, and CEBPB as the most likely transcription factors for mediating the function of SPHK1 (Fig. S6B). We determined the mRNA and protein levels of IRF-1, ATF-3, and CEBPB by RT-qPCR (Fig. S6C) and Western blot (Fig. S6D), and the results show that the mRNA and protein expression of ATF3 was increased after overexpression of SPHK1 in U251 cells

(Fig. S6D). Results from *in silico* analysis of TCGA data also showed that SPHK1 was highly correlated with PTX3 (Fig. 6B), suggesting that ATF3 mediated the regulatory effect of SPHK1 on PTX3 expression. A confocal immunofluorescence assay revealed co-localization of SPHK1 with ATF3 and ATF3 with PTX3 in the nuclei of both U251-MG and U87-MG cells (Fig. 6C). Next, a chromatin-immunoprecipitation (ChIP)-qPCR assay was used to confirm whether ATF3 could directly bind to the promoter of *PTX3*. As shown in Fig. 6D−F, we observed increased amounts of *PTX3* promoter DNA in cells overexpressing SPHK1 compared with control cells. A confocal immunofluorescence assay revealed that overexpression of ATF3 increased PTX3 expression in U251-MG cells (Fig. 6G). Rescue experiments also confirmed that silencing ATF3 impaired the effects of SPHK1 on release of PTX3, colony formation, 3D growth, and the ratio of p-STAT3/STAT3 in U251-MG cells (Fig. 6H−K and Supporting Information Fig. S7A), suggesting that PTX3 is a direct downstream target of ATF3 in GBM cells. Taken together, these results suggest that SPHK1-actived ATF3 binds to the promoter of PTX3 to regulate its expression.

3.7. *SPHK1 activates ATF3 through the JNK pathway*

To investigate how SPHK1 regulates the expression of ATF3, we tested whether several S1PR-related signaling pathways, including the MAPK, ERK, and JNK pathways, were involved in ATF3 expression mediated by SPHK1 (Fig. 7A). Overexpression of SPHK1 significantly increased the ratios of p-ERK/ERK and p-JNK/JNK in U251 cells (Fig. 7B). In contrast, knockdown of SPHK1 in A172 cells reduced the ratios of p-ERK/ERK, p-JNK/JNK, and p-JUN/JUN in U87-MG (Fig. 7C). However, p-p38-MAPK/p-38-MAPK was not changed when SPHK1 was overexpressed in GBM cells (Fig. 7C). We then treated U251-MG cells with the ERK inhibitor, PD98059, or the JNK inhibitor, SP600125, and found that SP600125 but not PD98059 suppressed the expression levels of p-STAT3/STAT3, ATF3, PTX3, IL-6, and the tumor spheroid formation ability in U251-MG cells (Fig. 7D−G and Supporting Information Fig. S7). Only SP600125 was able to rescue the effect of SPHK1 on the regulation of ATF3 and PTX3 and the tumor spheroid formation ability in U251-MG cells (Fig. 7F and G). In addition, to confirm that the activation of JNK by SPHK1 was caused by S1PRs rather than NF-κB activation, we detected the effects of the NF-κB inhibitor BAY11-7082 on the activation of JNK after overexpression of SPHK1 in U251-MG cells. Our results show that the phosphorylation of JNK was not changed after treatment of BAY11-7082 (Supporting Information Fig. S8). We speculate that the activation of JNK was caused by S1PR activation rather than NF-κB activation. Globally, these results suggest that SPHK1 activates ATF3 through the JNK/JUN pathway.

3.8. *SPHK1 interacts with PTX3 and forms a positive feedback loop to regulate inflammation and tumor growth of GBM cells*

To investigate whether SPHK1 interacted with PTX3, a co-immunoprecipitation (co-IP) assay was carried out. We found that SPHK1 and PTX3 were co-immunoprecipitated in U251-MG cells and GBM tissues, suggesting that SPHK1 interacted with PTX3 (Fig. 7H). An SPR assay using a Biacore ×100 instrument showed that PTX3 bound to SPHK1 with a K_d value is 2.98 μmol/L (Supporting Information Fig. S9). In addition, immunofluorescence results showed that SPHK1 and PTX3 were co-localized in the cytoplasm and nucleus in U251-MG and U87-MG cells (Fig. 4E). These results suggest that there is an interaction between SPHK1 and PTX3.

Additionally, the expression of ATF3, p-JNK/JNK and p-JUN/JUN were upregulated after overexpression of PTX3 in U251-MG cells (Fig. 7J and K), and were also increased after overexpression of SPHK1. PTX3 also increased the expression of SPHK1 (Fig. 7J). Taken together, these results suggest that SPHK1 and PTX3 may interact to form a positive feedback loop which can promote mutual expression, inflammation, and growth of GBM.

3.9. *SPHK1 promotes tumorigenesis; SPHK1 inhibition suppresses tumorigenesis*

To assess the role of SPHK1 in increasing the growth of tumors *in vivo*, stable cell lines with SPHK1 overexpression or knockdown were transplanted into nude mice (Fig. 8A). Tumor growth was monitored, and overexpression of SPHK1 increased tumor volume, tumor weight (Fig. 8B), the expression of PTX3, and the levels of S1P in tumor and serum (Fig. 8C) compared to control, confirming that SPHK1 promotes the growth of U251-MG cells in nude mice, while SPHK1 knockdown suppresses tumor growth, SPHK1 expression and the S1P level (Fig. 8D and E). To determine if SPHK1 could be a potential drug target for GBM therapy, a specific inhibitor of SPHK1, PF543, was tested in the GBM orthotopic model. Many studies have shown that PF543 is effective in mitigating bronchopulmonary dysplasia[24], high blood pressure[25], gastric cancer[26], prostate cancer[27] and breast cancer[28]. Here, we show that PF543 (10 mg/kg) significantly reduced tumor volume, the expression of PTX3, and the S1P level in mice transplanted with U87-MG cells (Fig. 8F and G) or U251-MG SPHK1 cells in an orthotopic model (Fig. 8H and I). These results provide evidence that SPHK1 could be a drug target in treating GBM.

4. Discussion

GBM is the most malignant type of brain tumor and TMZ is the only first-line drug, but it is not very effective. The molecular mechanism of GBM tumorigenesis is unclear and potential drug targets have not been identified. We found that SPHK1 was upregulated in GBM compared to normal tissues, and SPHK1 overexpression promoted growth and metastasis of GBM cells. SPHK1 induced inflammation through the NF-κB and IL-6/STAT3 pathways and promoted growth of GBM through the JUN/ATF3-mediated PTX3 pathway. SPHK1 interacted with PTX3 to form a positive feedback loop to mutually increase expression in GBM cells. Based on these results, SPHK1 may be a drug target for GBM treatment.

Inflammation is associated with the initiation, development, and progression of many cancers[29−32]. A previous study showed that S1P, a bioactive molecule induced by SPHK1, activated STAT3 and increased the expression of NF-κB and IL-6 in a colitis-associated mouse colon cancer model. Consistent with the previous study, we observed that overexpression of SPHK1 activated STAT3 and p65-NF-κB and increased IL-6 in GBM cells. IL-6 plays a crucial role in the development of GBM. Weissenberger et al.[33] demonstrated that abrogation of IL-6 prevented development of GBM in GFAP-v-src transgenic mice. Subsequent activation of JAK family members JAK1-3 leads to the activation of transcription factor STAT3. STAT3 promotes migration and invasion of U87MG, U251, and T98G GBM cells[34] and increases the expression of MMP-2, a protease involved in tumor metastasis[30,35]. IL-6/STAT3 also promotes proliferation and

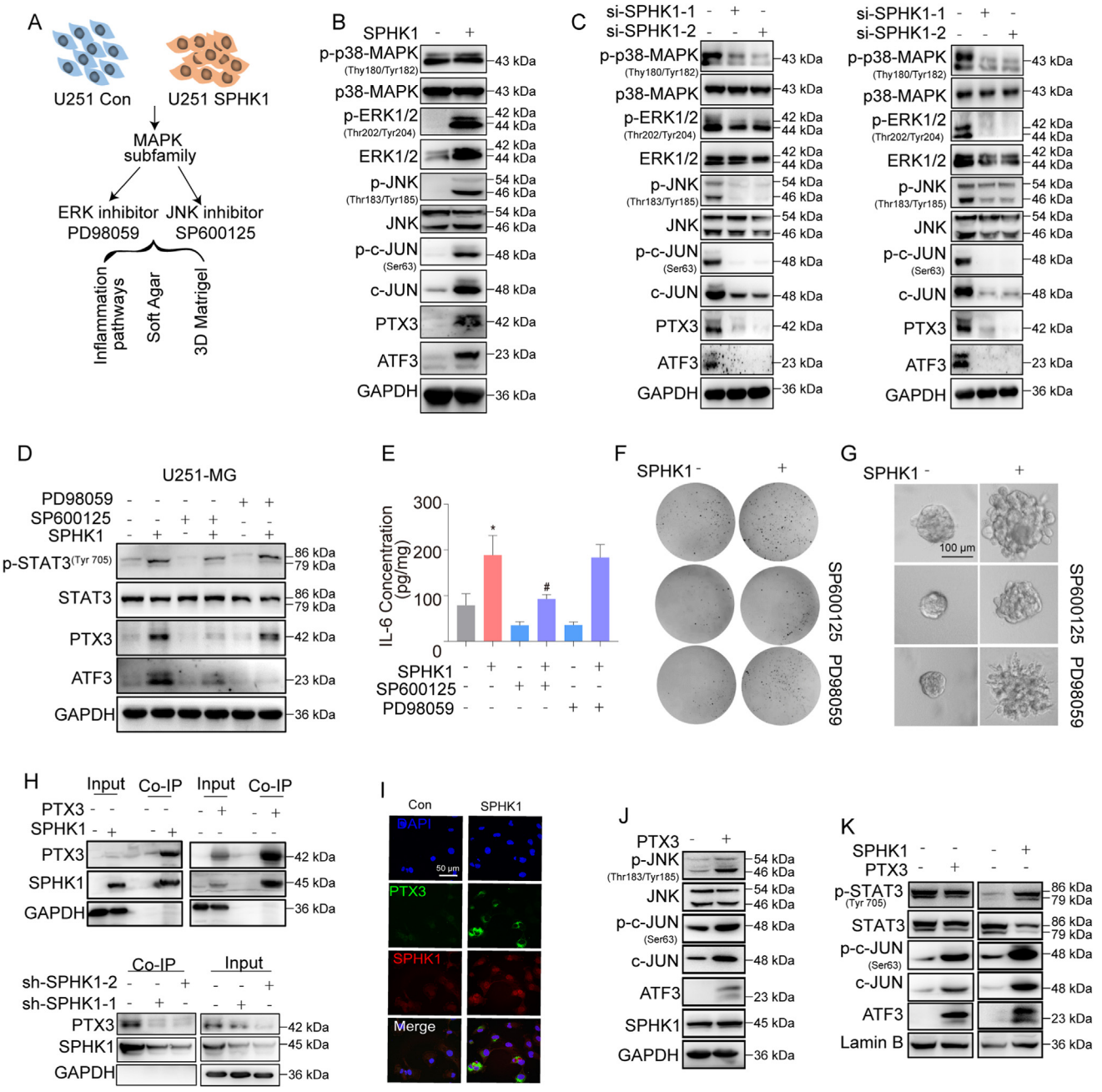

Figure 7 SPHK1 activates ATF3 through the JNK pathway and directly interacts with PTX3. (A) Strategy for identifying which pathway mediates the effects of SPHK1 on the regulation of PTX3. (B) Western blot results show that overexpression of SPHK1 increases the ratio of p-ERK/ERK and p-JNK/JNK in U251 cells. (C) Western blot results show that knockdown of SPHK1 and A172 cells reduces the ratio of P-ERK/ERK, p-JNK/JNK, and p-JUN/JUN in A172 and U87 cells. (D) The JNK inhibitor, SP600125, but not the ERK inhibitor, PD98059, suppresses expression of p-STAT3/STAT3, ATF3, and PTX3 after overexpression of SPHK1 in U251-MG cells. The JNK inhibitor, SP600125, but not the ERK inhibitor, PD98059, suppresses the release of IL-6 (E), colony formation (F) and growth in 3D Matrigel (G) in U251-MG cells after overexpression of SPHK1. (H) Co-IP analysis shows that SPHK1 and PTX3 co-immunoprecipitated in U251-MG cells and GBM tissues. (I) Confocal immunofluorescence results show that SPHK1 and PTX3 co-localize in the cytoplasm and nuclei in U251-MG cells. (J) Overexpression of PTX3 increases the expression of ATF3, p-JUN/JUN, and p-JNK/JNK in U251 cells. (K) Overexpression of SPHK1 or PTX3 increases the expression of ATF3, p-JUN/JUN, and p-STAT3/STAT3 in the nuclei of U251 cells. The data are presented as mean ± SD, and the experiments were performed in triplicate.

inhibits apoptosis of GBM cells[36]. Moreover, a recent study reports that vascular niche-derived IL-6 induces alternative *Mφ* activation in GBM, suggesting that IL-6 may serve as a therapeutic target for GBM immunotherapy[37], Inhibition of IL-6 by gene knockout or target drug modestly improves GBM T-cell infiltration and mouse survival rate[38].

Pentraxin 3 (PTX3) is a member of the pentraxin protein family and its concentration reflects the severity of inflammation.

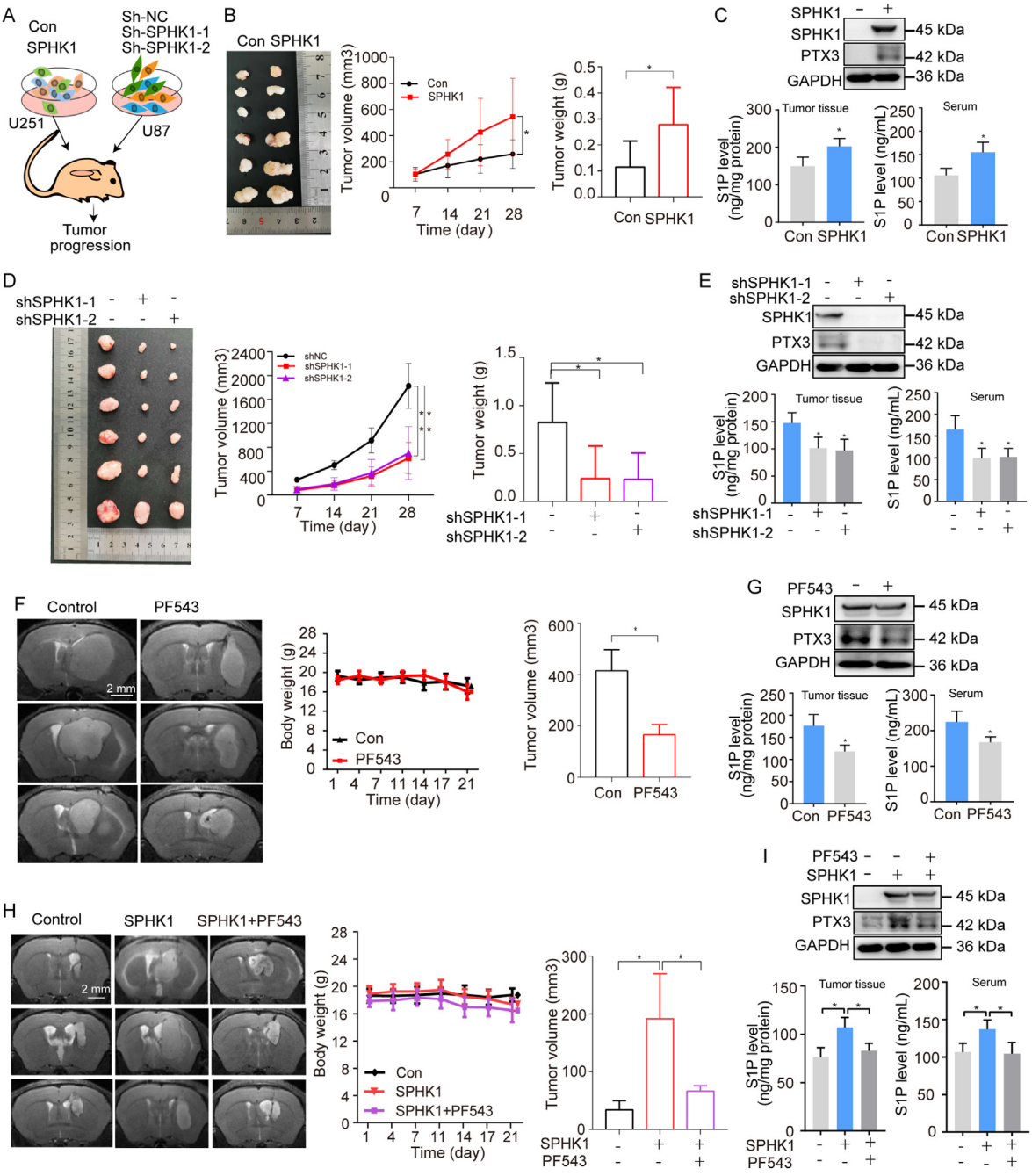

Figure 8 SPHK1 promotes tumor growth and SPHK1 inhibitor, PF543, suppresses tumorigenesis *in vivo*. (A) Strategy for studying the tumor promotion effects of SPHK1 *in vivo*. (B) Overexpression of SPHK1 in U251-MG cells increases tumor volume and weight in nude mice. The data are presented as mean ± SD, $n = 6$ in each group. (C) Overexpression of SPHK1 in U251-MG cells increases the expression of PTX3 and S1P levels in nude mice. The data are presented as mean ± SD, $n = 3$ in each group. (D) Knockdown of SPHK1 in U87-MG cells suppresses tumor growth in nude mice. The data are presented as mean ± SD, $n = 6$ in each group. (E) Knockdown of SPHK1 in U87-MG cells decreases the expression of PTX3 and S1P levels in nude mice. The data are presented as mean ± SD, $n = 3$ in each group. (F) PF543 significantly reduces tumor volume in mice transplanted with U87-MG cells in the orthotopic model. The data are presented as mean ± SD, $n = 3$ for MRI and tumor volume and $n = 6$ for body weight. (G) PF543 significantly reduces the expression of PTX3 and S1P levels in mice transplanted with U87-MG cells in the orthotopic model. The data are presented as mean ± SD, $n = 3$ in each group. (H) PF543 significantly inhibits tumor growth in mice transplanted with U251-MG SPHK1 cells in the orthotopic model. The data are presented as mean ± SD, $n = 3$ in each group. (I) PF543 significantly reduces the expression of PTX3 and S1P levels in mice transplanted with U251-MG SPHK1 cells in the orthotopic model. The data are presented as mean ± SD, $n = 3$ for MRI and tumor volume and $n = 6$ for body weight.

A previous study showed that PTX3 expression was upregulated and closely correlated with tumor progression in pancreatic carcinoma, cervical, prostate, gastric, and breast cancers and lung carcinoma[39]. PTX3 may promote invasion through enhanced angiogenesis in the GBM microenvironment through the IL8−VEGF signaling pathway[40]. In addition, silencing PTX3

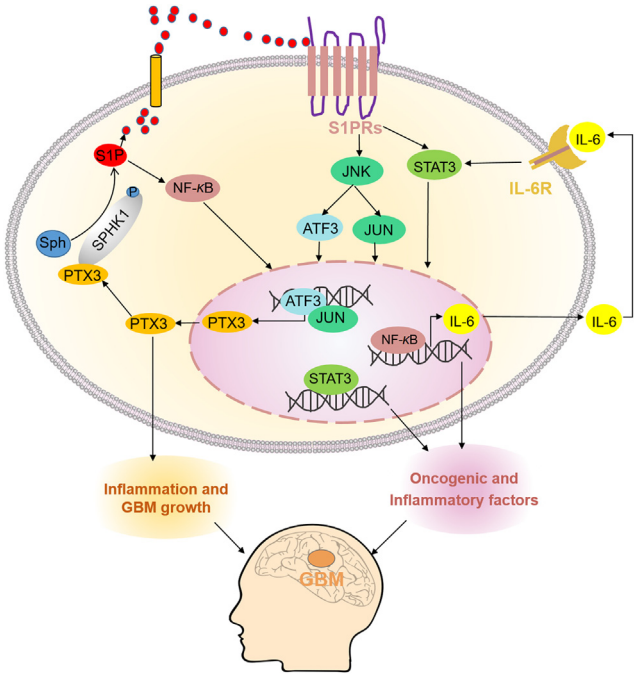

Figure 9 Diagram showing the proposed mechanism of SPHK1 action in GBM cells. SPHK1 promotes growth of GBM by increasing inflammation mediated by the NF-κB/IL-6/STAT3 and JNK/PTX3 pathways.

reduced the expression of VEGF and MMP-1[41]. PTX3 can also inhibit the expression of fibroblast growth factor two in rheumatoid arthritis[42]. We speculated that PTX3 may mediate the proliferation and motility of GBM cells through increased levels of growth factor and chemotactic receptors in GBM cells. Here, we report that SPHK1 increased the expression of PTX3 in GBM cells and show that PTX3 may be the main downstream gene target of SPHK1.

To clarify how SPHK1 increased the expression of PTX3, we determined if specific transcription factors were involved in PTX3 expression that was mediated by SPHK1. ATF3 is an important transcription factor that regulates the expression of many genes involved in cell cycle, apoptosis, and inflammation. We considered ATF3 as a putative mediator of SPHK1 and PTX3 because S1P binds to its receptors, S1PR1 or S1PR5, and then activates the MAPK signaling pathway, which is the upstream signal for ATF3. Also, our *in silico* analysis showed that the PTX3 promoter has an ATF3 binding site. Our results demonstrate that SPHK1 increased the expression of ATF3, and the ChIP-PCR data show that ATF3 was bound to the PTX3 promoter. This suggests that SPHK1 enhances the expression of PTX3 through transcriptional activation by ATF3 binding in GBM.

ATF3 is induced by pro-inflammatory cytokines, glucose, and other stimuli[43]. It is regulated by the NF-κB, STAT3, SAPK, and MAPK sub-family signaling pathways[44,45] depending on the stimulus[46]. In the present work, we observed increased phosphorylation of p38 MAPK, ERK, and JNK after overexpression of SPHK1. Using the ERK inhibitor, PD98059, and the JNK inhibitor, SP600125, we determined if JNK activation was required for SPHK1-induced ATF3. Our findings indicate that the JNK pathways rather than the p38 MAPK or ERK pathways were the upstream regulators of ATF3 induced by SPHK1. Previous results showed that ATF3 exerted its function by forming homodimers or heterodimers with other family members. For example, in the central nervous system, c-Jun was an important partner of ATF3 and a potential inducer of ATF3 expression. ATF3 and c-Jun can form heterodimers in reticulocytes[47], PC12 cells[48,49], and Neuro-2a cells[49]. In addition, as the key transcription factor, ATF3 interacts with other transcription factors, such as JUN, Sp1, and STAT3, in response to nerve injury[50,51]. Previous results also showed that PTX3 was transcriptionally regulated by JUN in breast cancer cells, and correlated with breast cancer stem-like properties[52]. We found that overexpression of SPHK1 increased the expression of JUN, which is also a downstream transcription factor in the JNK signaling pathway. Considering this evidence, we speculate that the bioactive product of SPHK1 is bound to its receptor and phosphorylates JNK to increase the expression of ATF3 and JUN. Subsequently, ATF3 interacts with JUN to form heterodimers to increase the expression of PTX3 in GBM cells.

Lastly, we found that SPHK1 could interact with PTX3 and co-localize with it in the cytoplasm and nucleus of U251-MG and U87-MG cells. Overexpression of PTX3 increased the expression of JNK, JUN and ATF3, which were also increased by overexpression of SPHK1. These findings indicate that SPHK1 and PTX3 established a positive feedback loop to reciprocally increase their expression, inflammation, and GBM proliferation.

5. Conclusions

We found that SPHK1 expression was upregulated in GBM tissues and cells and its expression was strongly associated with poor overall survival of patients with GBM. SPHK1 promoted the development of GBM by activating the JNK−JUN/ATF3 pathway, which transcriptionally regulated the expression of PTX3 and increased inflammatory processes and tumor progression. In addition, SPHK1 interacted with PTX3 to create a positive feedback loop that regulates the process of inflammation and tumorigenesis (Fig. 9). These results suggest that SPHK1 promotes the progression of GBM and may be useful as a therapeutic target for GBM therapy.

Acknowledgments

This work was supported by Beijing Natural Science Foundation (7212157, China). This work was also supported by CAMS Innovation Fund for Medical Sciences (2021-I2M-1-029 and 2022-12M-JB-011, China) and National Natural Science Foundation of China (81703536, China).

Author contributions

Wan Li performed most of the experiments, analyzed the data and wrote the draft. Hongqing Cai performed IHC assays. Hong Yang and Xiangjin Zheng designed the primers and performed qPCR. Jinyi Liu and Sha Li assisted in animal experiments. Liwen Ren and Yihui Yang carried out the Western blotting. Yizhi Zhang and Wei Tan carried out the data analysis. Jinhua Wang and Guanhua Du designed the project and revised the draft.

Conflicts of interest

The authors declare that there are no conflicts of interest.

Appendix A. Supporting information

Supporting data to this article can be found online at https://doi.org/10.1016/j.apsb.2022.09.012.

References

1. Stupp R, Hegi ME, Mason WP, van den Bent MJ, Taphoorn MJ, Janzer RC, et al. Effects of radiotherapy with concomitant and adjuvant temozolomide *versus* radiotherapy alone on survival in glioblastoma in a randomised phase III study: 5-year analysis of the EORTC-NCIC trial. *Lancet Oncol* 2009;**10**:459–66.
2. Stupp R, Mason WP, van den Bent MJ, Weller M, Fisher B, Taphoorn MJ, et al. Radiotherapy plus concomitant and adjuvant temozolomide for glioblastoma. *N Engl J Med* 2005;**352**:987–96.
3. Hemmati HD, Nakano I, Lazareff JA, Masterman-Smith M, Geschwind DH, Bronner-Fraser M, et al. Cancerous stem cells can arise from pediatric brain tumors. *Proc Natl Acad Sci U S A* 2003;**100**:15178–83.
4. Singh AB, Tsukada T, Zent R, Harris RC. Membrane-associated HB-EGF modulates HGF-induced cellular responses in MDCK cells. *J Cell Sci* 2004;**117**:1365–79.
5. Lee J, Kotliarova S, Kotliarov Y, Li A, Su Q, Donin NM, et al. Tumor stem cells derived from glioblastomas cultured in bFGF and EGF more closely mirror the phenotype and genotype of primary tumors than do serum-cultured cell lines. *Cancer Cell* 2006;**9**:391–403.
6. Giese A, Bjerkvig R, Berens ME, Westphal M. Cost of migration: invasion of malignant gliomas and implications for treatment. *J Clin Oncol* 2003;**21**:1624–36.
7. Hannun YA, Obeid LM. Principles of bioactive lipid signalling: lessons from sphingolipids. *Nat Rev Mol Cell Biol* 2008;**9**:139–50.
8. Ruckhaberle E, Rody A, Engels K, Gaetje R, von Minckwitz G, Schiffmann S, et al. Microarray analysis of altered sphingolipid metabolism reveals prognostic significance of sphingosine kinase 1 in breast cancer. *Breast Cancer Res Treat* 2008;**112**:41–52.
9. Song L, Xiong H, Li J, Liao W, Wang L, Wu J, et al. Sphingosine kinase-1 enhances resistance to apoptosis through activation of PI3K/Akt/NF-kappaB pathway in human non-small cell lung cancer. *Clin Cancer Res* 2011;**17**:1839–49.
10. Grivennikov SI, Greten FR, Karin M. Immunity, inflammation, and cancer. *Cell* 2010;**140**:883–99.
11. O'Callaghan DS, O'Donnell D, O'Connell F, O'Byrne KJ. The role of inflammation in the pathogenesis of non-small cell lung cancer. *J Thorac Oncol* 2010;**5**:2024–36.
12. Mantovani A, Allavena P, Sica A, Balkwill F. Cancer-related inflammation. *Nature* 2008;**454**:436–44.
13. Lin YJ, Wei KC, Chen PY, Lim M, Hwang TL. Roles of neutrophils in glioma and brain metastases. *Front Immunol* 2021;**12**:701383.
14. Wang J, Tang W, Yang M, Yin Y, Li H, Hu F, et al. Inflammatory tumor microenvironment responsive neutrophil exosomes-based drug delivery system for targeted glioma therapy. *Biomaterials* 2021;**273**:120784.
15. Xu K, Shu HK. EGFR activation results in enhanced cyclooxygenase-2 expression through p38 mitogen-activated protein kinase-dependent activation of the Sp1/Sp3 transcription factors in human gliomas. *Cancer Res* 2007;**67**:6121–9.
16. Van Brocklyn JR, Jackson CA, Pearl DK, Kotur MS, Snyder PJ, Prior TW. Sphingosine kinase-1 expression correlates with poor survival of patients with glioblastoma multiforme: roles of sphingosine kinase isoforms in growth of glioblastoma cell lines. *J Neuropathol Exp Neurol* 2005;**64**:695–705.
17. Kapitonov D, Allegood JC, Mitchell C, Hait NC, Almenara JA, Adams JK, et al. Targeting sphingosine kinase 1 inhibits Akt signaling, induces apoptosis, and suppresses growth of human glioblastoma cells and xenografts. *Cancer Res* 2009;**69**:6915–23.
18. Li M, Xu H, Wang J. Optimized functional and structural design of dual-target LMRAP, a bifunctional fusion protein with a 25-amino-acid antitumor peptide and GnRH Fc fragment. *Acta Pharm Sin B* 2020;**10**:262–75.
19. Chen Q, Li Q, Liang Y, Zu M, Chen N, Canup BSB, et al. Natural exosome-like nanovesicles from edible tea flowers suppress metastatic breast cancer *via* ROS generation and microbiota modulation. *Acta Pharm Sin B* 2022;**12**:907–23.
20. Wang J, Huang SK, Marzese DM, Hsu SC, Kawas NP, Chong KK, et al. Epigenetic changes of EGFR have an important role in BRAF inhibitor-resistant cutaneous melanomas. *J Invest Dermatol* 2015;**135**:532–41.
21. Gao X, You J, Gong Y, Yuan M, Zhu H, Fang L, et al. WSB1 regulates c-Myc expression through beta-catenin signaling and forms a feed-forward circuit. *Acta Pharm Sin B* 2022;**12**:1225–39.
22. Yu Q, Wu C, Chen Y, Li B, Wang R, Huang R, et al. Inhibition of LIM kinase reduces contraction and proliferation in bladder smooth muscle. *Acta Pharm Sin B* 2021;**11**:1914–30.
23. Li W, Ren L, Zheng X, Liu J, Wang J, Ji T, et al. 3-*O*-Acetyl-11-keto-beta-boswellic acid ameliorated aberrant metabolic landscape and inhibited autophagy in glioblastoma. *Acta Pharm Sin B* 2020;**10**:301–12.
24. Ha AW, Sudhadevi T, Ebenezer DL, Fu P, Berdyshev EV, Ackerman SJ, et al. Neonatal therapy with PF543, a sphingosine kinase 1 inhibitor, ameliorates hyperoxia-induced airway remodeling in a murine model of bronchopulmonary dysplasia. *Am J Physiol Lung Cell Mol Physiol* 2020;**319**:L497–512.
25. Jozefczuk E, Nosalski R, Saju B, Crespo E, Szczepaniak P, Guzik TJ, et al. Cardiovascular effects of pharmacological targeting of sphingosine kinase 1. *Hypertension* 2020;**75**:383–92.
26. Brew T, Bougen-Zhukov N, Mitchell W, Decourtye L, Schulpen E, Nouri Y, et al. Loss of E-cadherin leads to druggable vulnerabilities in sphingolipid metabolism and vesicle trafficking. *Cancers* 2021;**14**:102.
27. Lin HM, Mak B, Yeung N, Huynh K, Meikle TG, Mellett NA, et al. Overcoming enzalutamide resistance in metastatic prostate cancer by targeting sphingosine kinase. *EBioMedicine* 2021;**72**:103625.
28. Hii LW, Chung FF, Mai CW, Yee ZY, Chan HH, Raja VJ, et al. Sphingosine kinase 1 regulates the survival of breast cancer stem cells and non-stem breast cancer cells by suppression of STAT1. *Cells* 2020;**9**:886.
29. Kennedy BC, Showers CR, Anderson DE, Anderson L, Canoll P, Bruce JN, et al. Tumor-associated macrophages in glioma: friend or foe?. *JAMA Oncol* 2013;**2013**:486912.
30. Yeung YT, McDonald KL, Grewal T, Munoz L. Interleukins in glioblastoma pathophysiology: implications for therapy. *Br J Pharmacol* 2013;**168**:591–606.
31. Zhang J, Fan J, Zeng X, Nie M, Luan J, Wang Y, et al. Hedgehog signaling in gastrointestinal carcinogenesis and the gastrointestinal tumor microenvironment. *Acta Pharm Sin B* 2021;**11**:609–20.
32. Li M, Wang Y, Li M, Wu X, Setrerrahmane S, Xu H. Integrins as attractive targets for cancer therapeutics. *Acta Pharm Sin B* 2021;**11**:2726–37.
33. Weissenberger J, Loeffler S, Kappeler A, Kopf M, Lukes A, Afanasieva TA, et al. IL-6 is required for glioma development in a mouse model. *Oncogene* 2004;**23**:3308–16.
34. Li R, Li G, Deng L, Liu Q, Dai J, Shen J, et al. IL-6 augments the invasiveness of U87MG human glioblastoma multiforme cells *via* up-regulation of MMP-2 and fascin-1. *Oncol Rep* 2010;**23**:1553–9.
35. Liu Q, Li G, Li R, Shen J, He Q, Deng L, et al. IL-6 promotion of glioblastoma cell invasion and angiogenesis in U251 and T98G cell lines. *J Neuro Oncol* 2010;**100**:165–76.
36. Rahaman SO, Harbor PC, Chernova O, Barnett GH, Vogelbaum MA, Haque SJ. Inhibition of constitutively active Stat 3 suppresses proliferation and induces apoptosis in glioblastoma multiforme cells. *Oncogene* 2002;**21**:8404–13.
37. Wang Q, He Z, Huang M, Liu T, Wang Y, Xu H, et al. Vascular niche IL-6 induces alternative macrophage activation in glioblastoma through HIF-2 alpha. *Nat Commun* 2018;**9**:559.

38. Yang F, He Z, Duan H, Zhang D, Li J, Yang H, et al. Synergistic immunotherapy of glioblastoma by dual targeting of IL-6 and CD40. *Nat Commun* 2021;**12**:3424.
39. Giacomini A, Ghedini GC, Presta M, Ronca R. Long pentraxin 3: a novel multifaceted player in cancer. *Biochim Biophys Acta Rev Cancer* 2018;**1869**:53−63.
40. Wesley UV, Sutton I, Clark PA, Cunningham K, Larrain C, Kuo JS, et al. Enhanced expression of pentraxin-3 in glioblastoma cells correlates with increased invasion and IL8-VEGF signaling axis. *Brain Res* 2022;**1776**:147752.
41. Zhang JC, Tao T, Liu JQ. PTX3 promotes proliferation, invasion and drug resistance of neuroblastoma cells in children by regulating TLR4/NF-kappaB signaling pathway. *Chin J Oncol* 2021;**43**:118−25.
42. Zhao S, Wang Y, Hou L, Wang Y, Xu N, Zhang N. Pentraxin 3 inhibits fibroblast growth factor 2 induced osteoclastogenesis in rheumatoid arthritis. *Biomed Pharmacother* 2020;**131**:110628.
43. Hartman MG, Lu D, Kim ML, Kociba GJ, Shukri T, Buteau J, et al. Role for activating transcription factor 3 in stress-induced beta-cell apoptosis. *Mol Cell Biol* 2004;**24**:5721−32.
44. Rohini M, Haritha Menon A, Selvamurugan N. Role of activating transcription factor 3 and its interacting proteins under physiological and pathological conditions. *Int J Biol Macromol* 2018;**120**:310−7.
45. Nguyen CT, Kim EH, Luong TT, Pyo S, Rhee DK. TLR4 mediates pneumolysin-induced ATF3 expression through the JNK/p38 pathway in *Streptococcus pneumoniae*-infected RAW 264.7 cells. *Mol Cell* 2015;**38**:58−64.
46. Lu D, Chen J, Hai T. The regulation of *ATF3* gene expression by mitogen-activated protein kinases. *Biochem J* 2007;**401**:559−67.
47. Hai T, Curran T. Cross-family dimerization of transcription factors Fos/Jun and ATF/CREB alters DNA binding specificity. *Proc Natl Acad Sci U S A* 1991;**88**:3720−4.
48. Nakagomi S, Suzuki Y, Namikawa K, Kiryu-Seo S, Kiyama H. Expression of the activating transcription factor 3 prevents c-Jun N-terminal kinase-induced neuronal death by promoting heat shock protein 27 expression and Akt activation. *J Neurosci* 2003;**23**:5187−96.
49. Pearson AG, Gray CW, Pearson JF, Greenwood JM, During MJ, Dragunow M. ATF3 enhances c-Jun-mediated neurite sprouting. *Brain Res Mol Brain Res* 2003;**120**:38−45.
50. Hunt D, Raivich G, Anderson PN. Activating transcription factor 3 and the nervous system. *Front Mol Neurosci* 2012;**5**:7.
51. Kiryu-Seo S, Kato R, Ogawa T, Nakagomi S, Nagata K, Kiyama H. Neuronal injury-inducible gene is synergistically regulated by ATF3, c-Jun, and STAT3 through the interaction with Sp1 in damaged neurons. *J Biol Chem* 2008;**283**:6988−96.
52. Zhang P, Liu Y, Lian C, Cao X, Wang Y, Li X, et al. SH3RF3 promotes breast cancer stem-like properties *via* JNK activation and PTX3 upregulation. *Nat Commun* 2020;**11**:2487.